Nonlinear sorting, curvature generation, and crowding of Endophilin N-BAR on tubular membranes

Chen Zhu, Sovan L. Das, Tobias Baumgart

Supplementary Information

SUPPLEMENTARY METHODS

Preparation of Micropipettes Micropipettes (World Precision Instruments, Sarasota, FL) were manufactured with a pipette puller; pipette tips were clipped using a microforge. The inner opening diameters were 3-6 μm. Irreversible membrane/pipette adhesion was avoided by incubating micropipette tips with 0.5 mg/mL fatty-acid-free BSA dissolved in 1X PBS with a MicroFil needle (WPI), followed by rinsing, and pipettes were finally filled with 300 mM sucrose solution.

Preparation of chamber and tether pulling GUV dispersions obtained through electroswelling were diluted 1:10 in 300 mM sucrose solution. 50 μL diluted GUV dispersions, 0.5 μL 10X PBS, 0.5 μL streptavidin coated polystyrene bead solution and various concentrations of ENBAR-A488 (rat endophilin A1 N-BAR, amino acids 1-247, labeled at C108 with AlexaFluor 488) solution were injected into a measurement chamber. The chamber was constructed from microscope slides and coverslips that allowed access by two perpendicularly oriented micropipettes. Micropipettes were inserted into the chamber by a three-dimensional motorized manipulator system (Luigs and Neumann, Ratingen, Germany). Vesicles which were 10-25 μm in diameter were then selected which had enough excess area such that aspiration at initial pressures led to a projection with length larger than the pipette radius. Such a vesicle was pipette-aspirated with an initial suction pressure amounting to 5~10 Pa. The aspiration pressure was controlled by adjusting the water level of a reservoir connected to the micropipettes, and monitored by a pressure transducer with a DP-28 diaphragm (Validyne Engineering, Los Angeles, CA). In order to pull tethers, a second pipette was used to aspirate a bead at a pressure of ~50 Pa. The bead was gently moved toward the aspirated vesicle and contacted for ~1 min, and then moved away from the vesicle to pull a membrane tether of 5-15 μm in length, depending on vesicle size and excess area. All experiments were carried out at room temperature (20 ± 2 °C).

Measurement of tube radius The radii of membrane tubes displayed in Figs. 2 *E* and 2 *F* in the main text is below the resolution of the optical microscope. It is possible to estimate it after calibrating the fluorescence intensity measurements of tubes and vesicles via fluorescently labeled lipid (Ref. 38). The tube radius (R_t) is proportional to the fluorescence intensity from the lipid dye on the tube (I_t^{lipid}) normalized by the same intensity on the vesicle (I_v^{lipid}).

$$R_t = A \cdot \frac{I_t^{lipid}}{I_V^{lipid}} \tag{S1}$$

We experimentally determined the calibration factor A from a linear fit to a plot of the theoretically expected tube radius (varied through membrane tension, in the absence of protein) against this ratio, yielding a slope of A = 229 ± 40 nm (uncertainty is the standard deviation of three independent experiments). We then used this conversion factor to extract the tube radius from the curvature sorting experiments.

Error estimation of uncertainty in diffusion coefficient We use the χ–square test (Ref 48) to calculate uncertainties in diffusion coefficients. To calculate χ^2, we varied diffusion coefficients while fixing the fitting parameters ρ_0, as well as L_1 and L_2 (see main text for definitions of these parameters) and summed residuals according to

$$\chi(D_i(\Sigma))^2 = \sum_{j=1}^{n} \frac{[R(t_j)^{data} - R(t_j)_{D_i}^{fit}]^2}{\sigma^2} \tag{S2}$$

where σ is the relative uncertainty of the fluorescence intensity of an unbleached tether determined by image analysis, and D_i are values for the diffusion coefficient close to the optimal fit value. By calculating the following 2nd order differential, we obtained uncertainties s for the diffusion coefficients (see Fig. 3 *D*):

$$s = \sqrt{2/(\frac{\partial^2 \chi(D_i)^2}{\partial D_i^{\,2}})} \tag{S3}$$

Error estimation of uncertainty in fitting parameters for VdW model The uncertainties for fit parameters were determined by χ–square test. To obtain the uncertainty of the fit parameter a_i (i = 1-4 for a, b, θ_{ves} and C_p, respectively), we held $a_{k(k\neq i)}$ constant, and varied a_{ii} around a_i^{fit},

$$\chi(a_{ii})^2 = \sum_{j=1}^{n} \frac{[R(\Sigma_j)^{data} - R(\Sigma_j)_{a_{ii}}^{fit}]^2}{\sigma^2} \tag{S4}$$

where σ is the relative uncertainty of the fluorescence intensity as defined above. Calculating the 2nd order differential of χ^2 with respect to the parameter a_{ii} gives the uncertainty s_i for the fit parameter a_i:

$$s_i = \sqrt{2/(\frac{\partial^2 \chi(a_{ii})^2}{\partial a_{ii}^{\,2}})} \tag{S5}$$

Note that this approach neglects covariant terms in the error matrix.

Error propagation for membrane tension To estimate the uncertainty of membrane tension Σ (see Figs. 2 *C-F*), we used multivariate error analysis (Refs 31 and 48):

$$(\frac{\delta\Sigma}{\Sigma})^2 = (\frac{\delta(\Delta P)}{\Delta P})^2 + (\frac{R_v}{R_v - R_p})^2 (\frac{\delta R_p}{R_p})^2 + (\frac{R_p}{R_v - R_p})^2 (\frac{\delta R_v}{R_v})^2 \tag{S6}$$

The uncertainty of aspiration pressure ($\delta(\Delta P)$) was 0.5 Pa. Since the uncertainty in the pipette radius contributes a constant error to membrane tension(3), we ignored this component in our error analysis. The error for the vesicle radius (δR_v) was approximated as the image resolution, which is around 0.25 μm.

Determination of dissociation constant for ENBAR-A488 binding on GUVs Vesicles were prepared as described in the materials and methods section. GUV membranes contained 74% DOPC, 25% DOPG, 0.3% Texas Red-DHPE and 0.7% DSPE-Bio-PEG2000, and were incubated in 10 mM NaCl, 300 mM sucrose, 20 mM HEPES pH 7.4. Protein solutions were mixed with vesicles and incubated for 30 min before imaging. Vesicle fluorescence intensities were determined as described in the materials and methods section. Vesicle fluorescence intensity values as a function of protein solution concentration were fitted by a classical Langmuir adsorption isotherm.

TABLE S1 Fit parameters for protein sorting and tether radius measurements.

	[ENBAR] = 1 μM (Figs. 2 *C* and 2 *E*)	
	Non-dimensional	dimensional
a	0.00024 ± 0.0003	12.34 ± 16.5 k_BT·nm^2
b	0.0011 ± 0.00009	56.54 ± 4.4 nm^2
θ_{ves}	0.096 ± 0.004	0.096 ± 0.004
C_p	139.94 ± 7.2	0.14 ± 0.007 nm^{-1}
	[ENBAR] = 40 nM (Figs. 2 *D* and 2 *F*)	
	Non-dimensional	dimensional
a	0.0045 ± 0.0001	231.32 ± 7.1 k_BT·nm^2
b	0.0013 ± 0.00005	66.83 ± 2.8 nm^2
θ_{ves}	0.019 ± 0.0005	0.019 ± 0.0005
C_p	18.94 ± 0.2	0.019 ± 0.0002 nm^{-1}

The table lists the fit parameters resulting from simultaneously comparing the van der Waals curvature sorting model to the experimental protein sorting (Figs. 2 *C* and 2 *D*) and curvature generation (Figs. 2 *E* and 2 *F*) data. The uncertainties are estimated as described above.

SUPPLEMENTARY LEGENDS

FIGURE S1 Determination of the linear regime for detected fluorescence emission as a function of illumination power of 488 nm laser.
Green squares report green channel fluorescence; vertical line divides the range where detected emission is linearly proportional to excitation power. Red points show bleed-through into the red channel of ENBAR-A488 emission (for which lipid probe fluorescence intensity was corrected). $\Sigma = 0.15$mN/m.

FIGURE S2 Measurement of partitioning of reference lipid dye.
The figure shows linear dependency of fluorescence intensity of Texas Red-DHPE on the tube radii. The vesicle composition is 25 mol% DOPG, 74 mol% DOPC, 0.3 mol% TR-DHPE, and DSPE-Bio-PEG2000 content was 0.7 mol%. Extrapolation of the intensity plot linear fit approximately passed the origin of the graphs, demonstrating absence of detectable lipid sorting. Intercept in the figure is 0.44±31.66 (arbitrary units) (from three individual measurements). Error bars are standard error of mean for the three values from three experiments.

FIGURE S3 Dissociation constant K_d of ENBAR-A488 binding to GUVs.
ENBAR-A488 binding isotherm obtained from confocal fluorescence measurements (black dots), with standard deviations (gray vertical error bars) and standard errors of mean (black vertical error bar). A classical Langmuir isotherm fit to our data resulted in a dissociation constant K_d for ENBAR-A488 of 850 nM.

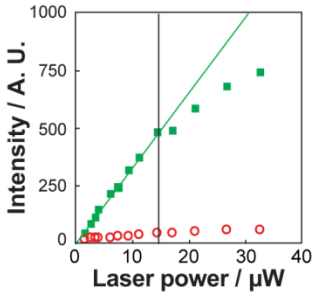

Figure S1

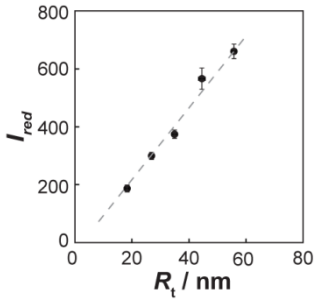

Figure S2

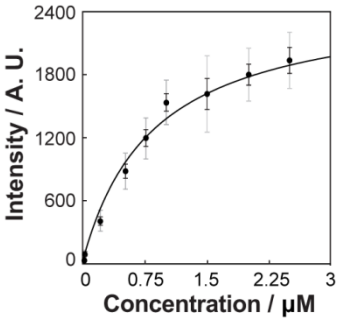
2400
1800
1200
600
0
Intensity / A. U.
0
0.75
1.5
2.25
3
Concentration / μM

Figure S3